



## Investigation of the pyrazinones as PDE5 inhibitors: Evaluation of regioisomeric projections into the solvent region

Robert O. Hughes<sup>a,\*</sup>, Todd Maddux<sup>a</sup>, D. Joseph Rogier<sup>a</sup>, Sharon Lu<sup>a</sup>, John K. Walker<sup>a</sup>, E. Jon Jacobsen<sup>a</sup>, Jeanne M. Rumsey<sup>a</sup>, Yi Zheng<sup>a</sup>, Alan MacInnes<sup>a</sup>, Brian R. Bond<sup>a</sup>, Seungil Han<sup>b</sup>

<sup>a</sup> Pfizer Global Research and Development, 700 Chesterfield Parkway West, St. Louis, MO 63017, USA

<sup>b</sup> Pfizer Global Research and Development, 100 Eastern Point Road, Groton, CT 06340, USA

### ARTICLE INFO

#### Article history:

Received 15 July 2011

Revised 19 August 2011

Accepted 25 August 2011

Available online 31 August 2011

#### Keywords:

PDE5 inhibitors

Pyrazinones

Lead optimization

Ligand efficiency

Lipophilic efficiency

### ABSTRACT

We describe the design, synthesis and profiling of a novel series of PDE5 inhibitors. We take advantage of an alternate projection into the solvent region to identify compounds with excellent potency, selectivity and pharmacokinetic profiles.

© 2011 Elsevier Ltd. All rights reserved.

Expressed in vascular smooth muscle cells phosphodiesterase type 5 (PDE5) hydrolyzes cGMP to the inactive metabolite 5'-GMP. Over the last decade, significant clinical and commercial experience has demonstrated the safety, tolerance and efficacy of PDE5 inhibitors, such as sildenafil, for the treatment of male erectile dysfunction (MED).<sup>1</sup> Recently, preclinical studies as well as clinical trials have suggested that PDE5 inhibitors could be/are effective in the treatment of various other diseases such as Raynaud's disease, gastrointestinal disorders and stroke.<sup>2</sup> Against this backdrop, we initiated a program directed toward the discovery of long-acting, selective inhibitors of PDE5.

We recently described the design, synthesis and evaluation of a series of aminopyridopyrazinones as novel PDE5 inhibitors (Fig. 1).<sup>3</sup> Optimization of the pharmacokinetic (PK) profile of advanced lead compound **1**, a highly potent and selective inhibitor of PDE5, led to cyclohexanol<sup>4</sup> **2** which had a favorable preclinical PK profile but attrited during rodent toxicological studies. Subsequent refinement led to the basic piperazine derivative **3** which is currently in clinical trials.<sup>5</sup> Herein, we describe our efforts to further examine the SAR of this series of compounds and develop alternate approaches to effectively balance the potency, selectivity and PK profiles. Examination of crystal structure of **1** (Fig. 4) bound to PDE5 suggested the geometric isomers envisioned in Figure 2 would project substituents into the solvent region and be well tolerated from

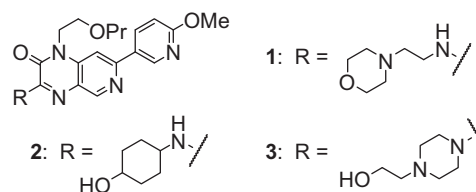


**Figure 1.** Key 1,3 aminopyrazinone lead structures: advanced lead **1**, pre-clinical candidate **2** and clinical candidate **3**.

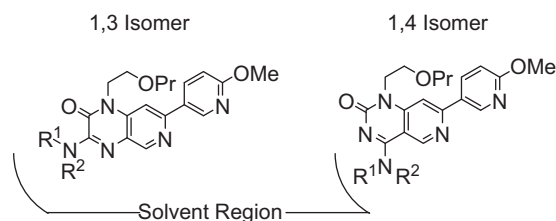
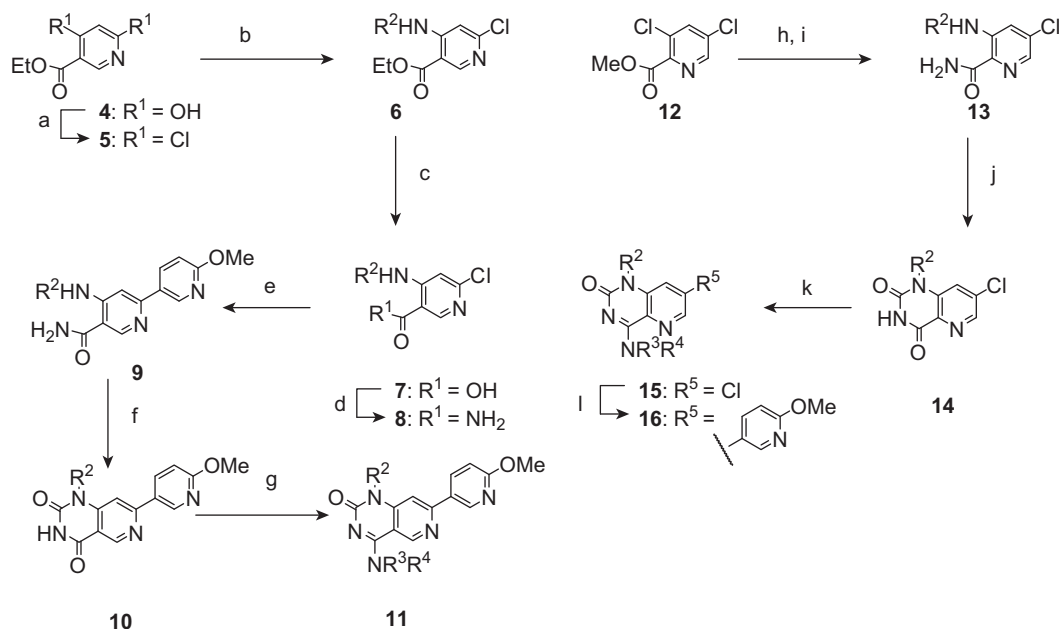


**Figure 2.** Proposed, novel 1,4 isomer compared to the 1,3 isomer. The southeastern pyridine<sup>6</sup> version of both cores is illustrated.

the potency perspective. Furthermore, we speculated that the 1,4 relationship between the propoxy ether and the solvent region may confer improved solubility as compared to the 1,3 derived compounds.

\* Corresponding author.

E-mail address: [robowenhughes@gmail.com](mailto:robowenhughes@gmail.com) (R.O. Hughes).



**Scheme 1.** Reagents and conditions: (a) POCl<sub>3</sub>, 100 °C; (b) R<sub>2</sub>NH<sub>2</sub>, dichloroethane, 23 °C; (c) LiOH, 1,2-dimethoxyethane, water, 23 °C; (d) SOCl<sub>2</sub>, cat. DMF, CH<sub>2</sub>Cl<sub>2</sub>, 23 °C then NH<sub>4</sub>OH (aq), 23 °C; (e) 6-methoxypyridin-3-ylboronic acid, Pd(Ph<sub>3</sub>P)<sub>4</sub>, Na<sub>2</sub>CO<sub>3</sub>, dioxane, water, reflux; (f) NaH, di(1*H*-imidazol-1-yl)methanone, DMF, 0→75 °C; (g) POCl<sub>3</sub>, 100 °C then R<sub>3</sub>R<sub>4</sub>NH, CH<sub>2</sub>Cl<sub>2</sub>, 23 °C; (h) 7 N NH<sub>3</sub>, MeOH, 23 °C; (i) R<sub>2</sub>NH<sub>2</sub>, *i*Pr<sub>2</sub>NEt, DMSO, 120 °C; (j) NaH, di(1*H*-imidazol-1-yl)methanone, DMF, 0→75 °C; (k) SOCl<sub>2</sub>, cat. DMF, CH<sub>2</sub>Cl<sub>2</sub>, 23 °C then R<sub>3</sub>R<sub>4</sub>NH, CH<sub>2</sub>Cl<sub>2</sub>, 23 °C; (l) 6-methoxypyridin-3-ylboronic acid, Pd(Ph<sub>3</sub>P)<sub>4</sub>, Na<sub>2</sub>CO<sub>3</sub>, dioxane, water, reflux.

To examine the potential of this geometry we synthesized several prototype compounds in both the southeastern and southern pyridine core ring systems. The syntheses of these rings systems are illustrated in Scheme 1. Synthesis of 1,4 southeastern pyridines (general structure **11**) commenced with the chlorination of dihydroxy pyridine **4** in neat POCl<sub>3</sub> to yield **5**. Displacement of the 4-chloro group in **5** with various primary amines proceeded smoothly and in good yield to give **6**. Saponification followed by formation of the primary amide gave **8** in nearly quantitative yield. Suzuki cross coupling between **8** and 6-methoxypyridin-3-ylboronic acid yielded **9** in 65% yield. Treatment of **9** with CDI and sodium hydride provided the penultimate dione, **10**, in excellent yield. Finally, chlorination of **10** with POCl<sub>3</sub> provided the highly reactive intermediate chloropyrimidinone which was immediately reacted with the requisite amines to give **11**. The synthesis of the southern pyridine derived isomers (**16**) proceeded along a similar synthetic route. We began from the known intermediate **12** which was converted to the analogous amide by the action of 7 N NH<sub>3</sub>. Treatment of this compound with primary amines in DMSO at 120 °C proceeded in modest yield to provide **13**. Treatment of amino amide **13** with CDI and sodium hydride provided **14**. Chlorination with SOCl<sub>2</sub> followed by displacement with amines afforded the aminopyrimidinones, **15**. The synthesis of **16** was completed via a Suzuki cross coupling (42% yield).

Table 1 summarizes the PDE5 potency and PDE6 and PDE11 selectivity and compares the characteristics of the 1,3 and 1,4 geometries in both the southeastern and southern pyridine cores. The PDE5 potency of the 1,4 geometry was similar to what we had determined for the 1,3 system. For instance, morpholines **1** (PDE5 IC<sub>50</sub> = 0.07 nM) and **17** (PDE5 IC<sub>50</sub> = 0.08 nM) were equipotent against PDE5 as were southeastern cyclohexanols **2** (PDE5 IC<sub>50</sub> = 0.05 nM) and **18** (PDE5 IC<sub>50</sub> = 0.05 nM). For both piperazine pairs (**3** and **21** and **22** and **23**) there was approximately a fivefold loss in potency in the 1,4 geometry as compared to the 1,3 geometry; however, both **21** and **23** possess nanomolar potency against PDE5 (IC<sub>50</sub> = 1.38 and 1.64 nM, respectively). We were further encouraged by the suggestion from this early set of compounds

**Table 1**

Comparison of the PDE5 potency and PDE6 and PDE11 selectivity of 1,3 southeastern and southern pyridines to 1,4 southeastern and southern pyridines

X	Core	-NR <sup>3</sup> R <sup>4</sup>	PDE5 <sup>a</sup>	6x/11x <sup>b</sup>
<b>1</b>	1,3SE		0.07	158/4860
<b>17</b>	1,4SE		0.08	334/9050
<b>2</b>	1,3SE		0.05	200/1316
<b>18</b>	1,4SE		0.05	675/3950
<b>19</b>	1,3S		0.32	48/675
<b>20</b>	1,4S		0.10	1020/3830
<b>3</b>	1,3SE		0.20	157/2463
<b>21</b>	1,4SE		1.38	181/>1450
<b>22</b>	1,3S		0.35	245/1771
<b>23</b>	1,4S		1.64	381/>1220

<sup>a</sup> PDE IC<sub>50</sub> (nM).

<sup>b</sup> 6x = PDE6 IC<sub>50</sub>/PDE5 IC<sub>50</sub>; 11x = PDE11 IC<sub>50</sub>/PDE5 IC<sub>50</sub>.

that the 1,4 geometry might afford more selectivity, particularly over PDE6, than the analogous 1,3 compound. For example, **20** is significantly more selective than **19** (1020-fold vs 48-fold).<sup>7</sup>

Encouraged by these early results we designed and synthesized a diverse library of compounds to rapidly establish the key features

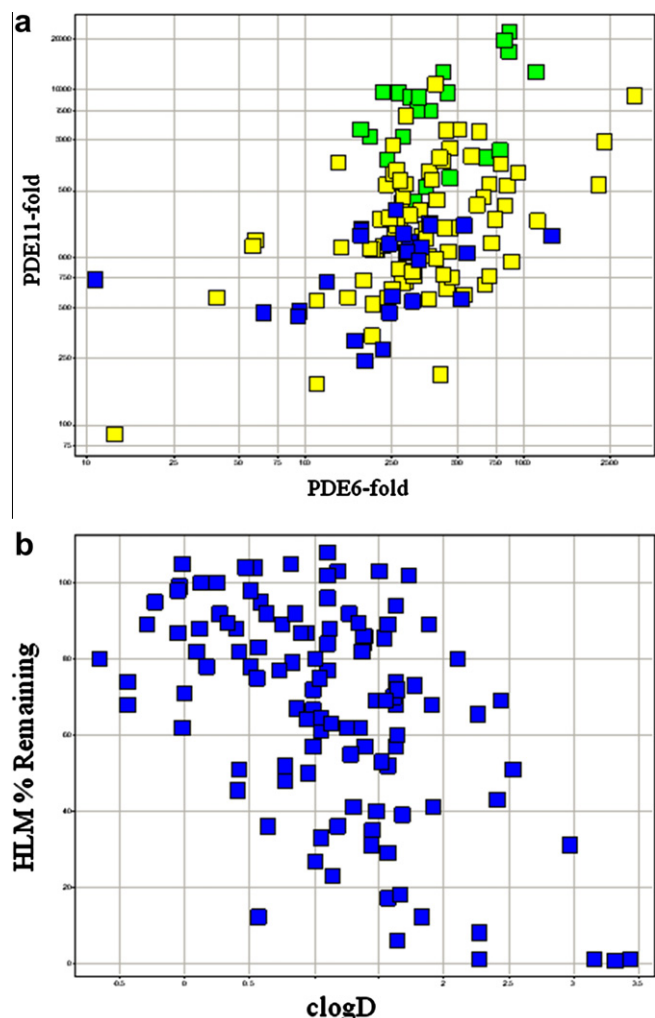


**Figure 3.** (a) Summarizes the selectivity and potency data of broad set of compounds examining the solvent region. Green boxes denote PDE5 IC<sub>50</sub> < 0.1 nM; yellow boxes 0.1 nM < PDE5 IC<sub>50</sub> < 1 nM; and blue boxes 1.0 nM < PDE5 IC<sub>50</sub>. (b) Illustrates the relationship between calculated logD and human liver microsomal stability. PDE11-fold and PDE6-fold refer to the ratio: PDE11 IC<sub>50</sub>/PDE5 IC<sub>50</sub> and PDE6 IC<sub>50</sub>/PDE5 IC<sub>50</sub>, respectively.

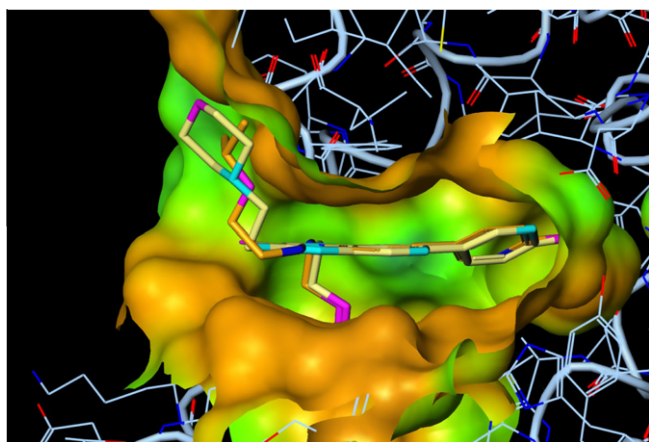


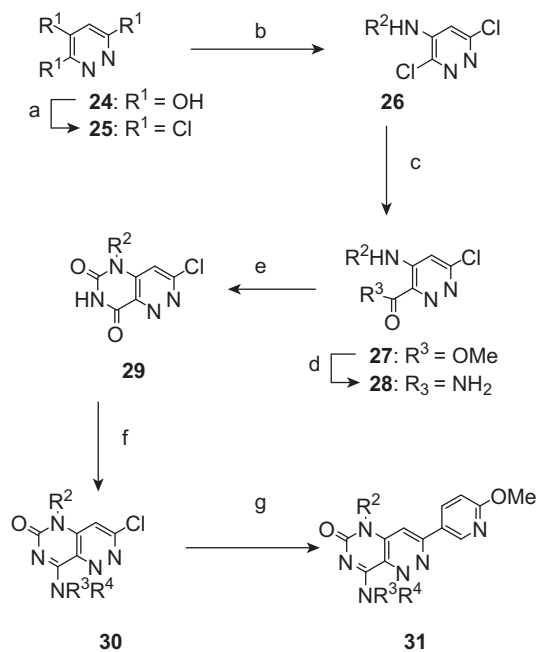
**Figure 4.** Crystallographic data for 1,3 analog **1** (yellow), bearing the morpholinoethylamino side chain, and a 1,4 analog (orange),<sup>9</sup> bearing the isopropoxyethyl amino side chain, bound to PDE5.

of the 1,4 geometry in the solvent region. We choose to conduct this evaluation utilizing the southeastern pyridine ring system

(**11**) as its synthesis allowed for the installation of the solvent region in the last step. The results for 115 compounds are summarized graphically in Figure 3. As shown in panel (a) of Figure 3, 82% of these compounds possessed PDE5 IC<sub>50</sub>s < 1 nM. Further, 98% of the compounds synthesized demonstrated both PDE6 and PDE11 selectivities greater than and 100-fold. Figure 4 shows crystallographic data<sup>8</sup> for both 1,3 (**1**) and 1,4 compound compounds bound to PDE5. In this instance, the two relatively flexible side-chains (ethyl morpholine and ethyl isopropoxyl) occupy a similar area of space. This observation explains the similar PDE5 potency findings between the two series. Moreover, this observation gave us the confidence to forgo a wide ranging potency optimization campaign for the 1,4 series as this would most likely only duplicate the efforts and results obtained during the optimization campaign for the 1,3 series. Instead we chose to focus our attention on incorporating the optimal groups identified during the optimization of the 1,3 system into the 1,4 series.

Figure 3, panel (b) illustrates the trend relating in vitro metabolic stability (human liver microsomes, percent remaining after one hour of incubation) to calculated lipophilicity (clogD). The probability of a compound displaying favorable metabolic stability increased steadily with reduced clogD. Specifically, the probability is 90% (clogD < 1), 70% (1 < clogD < 2) and 35% (clogD > 2). In order to increase the probability of finding compounds with an excellent potency, selectivity and metabolic stability profile, we sought core structural modifications which would retain high potency at lower lipophilicity. Accordingly we considered pyridazine ring systems such as **31** (see Scheme 2).

Synthesis of the pyridazines (general structure **31**) is summarized in Scheme 2 and initiated with known pyridazine-3,4,6-triol (**24**). Chlorination with POCl<sub>3</sub> give the relatively stable tri-chloro compound, **25**, from which the desired was chlorine was displaced by the action of primary amines in ethanol. As the key step, regioselective palladium-mediated carbonylation of **26** provided methyl ester **27** in 85% yield. Direct conversion to the primary amide, **28**, was brought about by treatment with 7 N NH<sub>3</sub> in



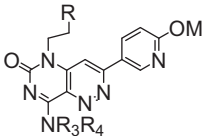
**Scheme 2.** Reagents and conditions: (a) POCl<sub>3</sub>, 100 °C; (b) R<sub>2</sub>NH<sub>2</sub>, ethanol, 0 °C; (c) CO, Pd(dppf)<sub>2</sub>, methanol, DMF, 80 °C; (d) 7 N NH<sub>3</sub>, MeOH, 0 → 23 °C; (e) NaH, di(1H-imidazol-1-yl)methanone, DMF, 0 → 75 °C; (f) oxalyl chloride, cat. DMF, dichloromethane, 0 → 23 °C then R<sub>3</sub>R<sub>4</sub>NH, CH<sub>2</sub>Cl<sub>2</sub>, 0 → 23 °C; (g) 6-methoxyppyridin-3-ylboronic acid, Pd(Ph<sub>3</sub>P)<sub>4</sub>, Na<sub>2</sub>CO<sub>3</sub>, dioxane, water, reflux.

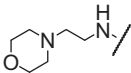
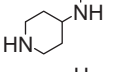
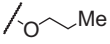
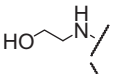
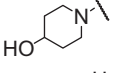
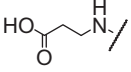
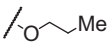
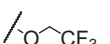
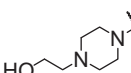
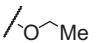
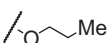
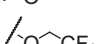
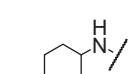
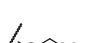
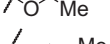
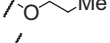
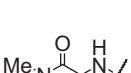
methanol. Cyclization of **28** with CDI gave **29**. The synthesis was completed in a similar manner as the southeastern and southern pyridine isomers. Specifically, chlorination of **29** with thionyl chloride followed by immediate treatment of the highly reactive chloropyrimidine with amines gave **30** which was converted to the final, desired product (**31**) via Suzuki cross-coupling.

Table 2 summarizes the PDE5 potency and PDE6 and PDE11 selectivity for a series of pyridazine-derived compounds. As anticipated from our initial scan of the solvent region (Fig. 3), a wide variety of substitution patterns were well tolerated in terms of both PDE5 potency and PDE6 and PDE11 selectivity. For instance, basic amines **32** (PDE5  $IC_{50}$  = 0.09 nM; PDE6 and PDE11 >500-fold) and **33** (PDE5  $IC_{50}$  = 1.31 nM; PDE6 and PDE11 >500-fold) and neutral alcohols such as **34** (PDE5  $IC_{50}$  = 0.22 nM; PDE6 and PDE11 >250-fold) and **35** (PDE5  $IC_{50}$  = 0.28 nM; PDE6 and PDE11 >200-fold) displayed an excellent in vitro profile. Interestingly, as carboxylic acids were not well-tolerated in the 1,3 geometry, **36** was observed to

**Table 2**

Summary of PDE5 potency and PDE6 and PDE11 selectivity for a series of 1,4 pyridazines



X	R	$-NR^3R^4$	PDE5 <sup>a</sup>	6x/11x <sup>b</sup>
32			0.09	573/6820
33			1.31	576/1530
34			0.22	290/240
35			0.28	194/240
36			0.05	139/250
37			1.30	124/834
38			0.64	818/>311
39			2.43	98/286
40			0.02	108/741
41			0.04	3620/11,400
42			0.36	125/506
43			0.44	296/277
44			0.38	2200/4170
45			1.47	119/199

<sup>a</sup> PDE  $IC_{50}$  (nM).

<sup>b</sup> 6x = PDE6  $IC_{50}$ /PDE5  $IC_{50}$ ; 11x = PDE11  $IC_{50}$ /PDE5  $IC_{50}$ .

have an excellent potency and selectivity profile. Interestingly, the increase in polarity of pyridazine (relative to the pyridine isomers) does not result in a loss of potency. Examination of the pair-matched set of 20 solvent groups, comparing the pyridazine core to the southeast pyridine core showed that the ligand efficiency<sup>10</sup> was similar (0.42 for the pyridazines and 0.41 for the southeast pyridine) but the lipophilic ligand efficiency<sup>11</sup> increased significantly (7.2 for the pyridazines and 6.5 for the southeast pyridine). This increase in lipophilic efficiency improved our ability to design potent, selective and metabolically stable molecules.

Analogs **37–45** were designed to probe the contributions to potency, selectivity and PK of the alkoxy substituent (see Table 2). Both less lipophilic groups, such as ethyl ethoxy, and metabolically-blocked groups, such as ethyl trifluoroethoxy, retained excellent potency and selectivity. Indeed, the ethyl trifluoroethoxy group afforded a significant improvement in PDE6 and PDE11 selectivity. The ethyl ethoxy group was somewhat less active than the ethyl propoxyloxy.

Table 3 summarizes the in vitro and in vivo PK properties of three analogs from the cyclohexanol series compared to the 1,3 compound **2**. All four compounds possessed excellent in vitro metabolic stability as judged by incubation with human liver microsomes. Furthermore, **40** and **42** demonstrated low clearance (<10 mL/min/kg), a low volume of distribution (1–2 L/kg) and high bioavailability (85–100%) in the these studies. Interestingly, the trifluoroethyl derivative, **41**, possessed a significantly higher clearance (36.5 mL/min/kg) and volume of distribution (4.8 L/kg). Comparison of the unbound clearance of **40** to **2** highlights the dramatic increase in intrinsic metabolic stability of **40**. Furthermore, **40** and **42** possessed improved solubility profiles as compared to **2**.

Based on its favorable potency, selectivity and pharmacokinetic profile, compound **40** was extensively profiled. As with compounds such as **2** and **3**, from the 1,3 series, **40** demonstrated excellent selectivity against the other members of the PDE family as well as against a wide panel of targets.<sup>12</sup> At 3  $\mu$ M, **40** did not significantly inhibit CYP2C9 (9%), CYP3A4 (23%) nor CYP2D6 (5%). In our pharmacodynamic model in the spontaneously hypertensive rat, **40** demonstrated robust blood pressure lowering (systolic BP  $\Delta$  = –20–30 mmHg) for >24 h following a single dose of 20 mpk. Additional studies indicated, as previously noted, that efficacy was maintained when trough, free plasma concentrations exceeded 10xPDE5  $IC_{50}$ . Taking this data together with the preclinical PK profile we predicted a human PK profile supportive of once-a-day dosing with a low dose of less than 5 mg. Additional data on **40** will be reported in due course.

**Table 3**

Summary of pharmacokinetic properties of **2**, **40**, **41** and **42**

Property	<b>2</b>	<b>40</b>	<b>41</b>	<b>42</b>
clogD	1.3	0.79	0.47	0.23
Solubility <sup>a</sup>	21	>100	34	>100
HLM <sup>b</sup>	84	72	100	63
Rat Cl <sup>c</sup>	5.5	2.4	36.5	9.4
Rat Cl <sub>u</sub>	392	19.2	ND	ND
Rat Vd <sup>d</sup>	1.35	0.6	4.8	1.3
Rat Vd <sub>u</sub>	96	4.8	ND	ND
Rat fu <sup>e</sup>	1.4	12.5	ND	ND
Rat% F <sup>f</sup>	50	85	73	100
Dog Cl <sup>c</sup>	5.5	1.6	ND	ND
Dog Vd <sup>d</sup>	3.5	0.3	ND	ND

<sup>a</sup> Solubility ( $\mu$ M) at pH 6.5.

<sup>b</sup> % remaining after 1 h in human liver microsomes.

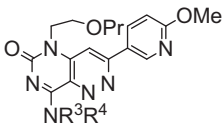
<sup>c</sup> Clearance in mL/min/kg; 2 mpk (n = 3) vehicle: 70% PEG400/20% 0.05 M citrate buffer/10% ethanol, pH 5.

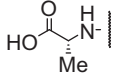
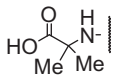
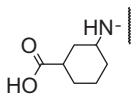
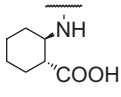
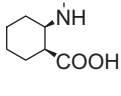
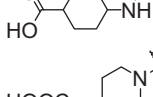
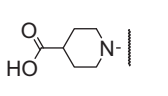
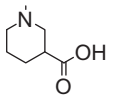
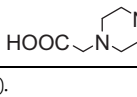
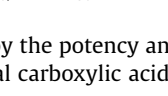
<sup>d</sup> Volume of distribution in L/kg.

<sup>e</sup> Fraction unbound.

<sup>f</sup> 2 mpk (n = 3) vehicle: 0.5% methylcellulose/0.1% Tween 80 in 50 mM citric acid, pH 5.

**Table 4**  
Summary of the PDE5 potency and PDE6 and PDE11 selectivity for a series of acidic analogs



X	-NR <sup>3</sup> R <sup>4</sup>	PDE5 <sup>a</sup>	6x/11x <sup>b</sup>
46		0.13	110/76
47		0.05	145/129
48		0.01	172/2090
49		0.27	47/1390
50		0.02	110/296
51		0.02	246/541
52		0.04	254/1060
53		0.01	119/532
54		0.06	162/297
55		0.10	143/1330

<sup>a</sup> PDE IC<sub>50</sub> (nM).

<sup>b</sup> 6x = PDE6 IC<sub>50</sub>/PDE5 IC<sub>50</sub>; 11x = PDE11 IC<sub>50</sub>/PDE5 IC<sub>50</sub>.

Intrigued by the potency and selectivity profile of **36** we evaluated additional carboxylic acid derivatives. The PDE5 potency and

PDE6 and PDE11 selectivity data for this set of compounds is summarized in Table 4. As observed with compound **36**, these compounds examined possessed sub-nanomolar PDE5 potency and an excellent selectivity profile. Interestingly, racemic stereoisomers **49** and **50** displayed somewhat disparate potency and selectivity profiles. The *trans*-isomer, **50**, was an order of magnitude less potent (PDE5 IC<sub>50</sub> = 0.27 nM) and less PDE6 selective but more PDE11 selective than the *cis*-isomer. Unfortunately, evaluation of this series of compounds in vivo suggested high, non-hepatic clearance. The rat PK for **48** is representative of the series: clearance = 195 mL/min/kg and %F = 17, following a 2 mpk iv and po dose. Efforts to improve the PK profile were not successful and the acidic sub-series was de-emphasized.

In summary, we have described the design and synthesis of a novel series of PDE5 inhibitors which exploited an alternate projection into the solvent region. Compound **40** was rapidly identified as an attractive lead molecule and was extensively profiled.

## References and notes

- Rashid, A. *Clin. Cornerstone* **2005**, *7*, 47.
- Sandner, P.; Huetter, J.; Tinel, H.; Ziegelbauer, K.; Bischoff, E. *Int. J. Impot. Res.* **2007**, *19*, 533.
- Hughes, R. O.; Walker, J. K.; Cabbage, J. W.; Fobian, Y. M.; Rogier, D. J.; Heasley, S. E.; Blevis-Bal, R. M.; Benson, A. G.; Owen, D. R.; Jacobsen, E. J.; Freskos, J. N.; Molyneaux, J. M.; Brown, D. L.; Stallings, W. C.; Acker, B. A.; Maddux, T. M.; Tollefson, M. B.; Williams, J. M.; Moon, J. B.; Mischke, B. V.; Rumsey, J. M.; Zheng, Y.; MacInnes, A.; Bond, B. R.; Yu, Y. *Bioorg. Med. Chem. Lett.* **2009**, *19*, 4092.
- Hughes, R. O.; Walker, J. K.; Joseph, R. D.; Heasley, S. E.; Blevis-Bal, R. M.; Benson, A. G.; Jacobsen, E. J.; Cabbage, J. W.; Fobian, Y. M.; Owen, D. R.; Freskos, J. N.; Molyneaux, J. M.; Brown, D. L.; Acker, B. A.; Maddux, T. M.; Tollefson, M. B.; Moon, J. B.; Mischke, B. V.; Rumsey, J. M.; Zheng, Y.; MacInnes, A.; Bond, B. R.; Yu, Y. *Bioorg. Med. Chem. Lett.* **2009**, *19*, 5209.
- Hughes, R. O.; Rogier, D. J.; Jacobsen, E. J.; Walker, J. K.; MacInnes, A.; Bond, B. R.; Zhang, L. L.; Yu, Y.; Zheng, Y.; Rumsey, J. M.; Walgren, J. L.; Curtiss, S. W.; Fobian, Y. M.; Heasley, S. E.; Cabbage, J. W.; Moon, J. B.; Brown, D. L.; Acker, B. A.; Maddux, T. M.; Tollefson, M. B.; Mischke, B. V.; Owen, D. R.; Freskos, J. N.; Molyneaux, J. M.; Benson, A. G.; Blevis-Bal, R. M. *J. Med. Chem.* **2010**, *53*, 2656.
- Southern and Southeastern pyridine refer to the location of the Nitrogen in the right-hand ring (as drawn) system. The propoxy group is on the 'northern' side of the ring system.
- Presently, we do not have a compelling structure-based rationale for this finding.
- PDB accession codes: 3TGE and 3TGG.
- Data for 4-[(2-isopropoxyethyl)amino]-7-(6-methoxypyridin-3-yl)-1-(2-propoxyethyl)pyrido[4,3-d]pyrimidin-2(1H)-one: PDE5 IC<sub>50</sub> = 0.1 nM; PDE6/PDE5 = 450-fold; PDE11/PDE5 = 9560-fold.
- Hopkins, L. A.; Groome, C. R.; Alex, A. *Drug Discovery Today* **2004**, *9*, 430.
- Ryckmans, T.; Edwards, M. P.; Horne, V. A.; Correia, A. M.; Owen, D. R.; Thompson, L. R.; Tran, I.; Tutt, M. F.; Young, T. *Bioorg. Med. Chem. Lett.* **2009**, *19*, 4406.
- For the PDE family we determined: PDE1A, PDE1B, PDE1C, PDE2, PDE3A, PDE3B, PDE4A, PDE4B, PDE4C, PDE7A, PDE7B, PDE8A, PDE8B, PDE9 and PDE10 IC<sub>50</sub> >2000 nM. Screening in the CEREP broad screen of >50 off-targets at 10 mM revealed only two weak hits: adenosine A1 IC<sub>50</sub> = 440 nM and acetylcholinesterase IC<sub>50</sub> = 5600 nM.